Co-ordination Fingerprints in Electron Loss Near-Edge Structures: Determination of the Local Site Symmetry of Aluminium and Beryllium in Ultrafine Minerals

R. Brydson,*[a] H. Sauer,[b] W. Engel,[b] J. M. Thomas,[c] and E. Zeitler[b]

[a] *The Blackett Laboratory, Imperial College of Science and Technology, Prince Consort Road, London SW7 2BZ, U.K.*
[b] *Fritz-Haber-Institut der Max-Planck-Gesellschaft, Faradayweg 4–6, D1000 Berlin 33 (Dahlem), Federal Republic of Germany*
[c] *Davy-Faraday Research Laboratory, The Royal Institution, 21 Albemarle Street, London W1X 4BS, U.K.*

The correlation of electron energy loss near-edge structures with specific nearest neighbour co-ordinations is demonstrated for aluminium and beryllium in two different minerals; the implications for routine microanalysis are discussed.

Recent improvements in instrumentation have stimulated renewed interest in the measurement of electron loss near-edge structures (ELNES) of inner shell excitations produced by high energy electrons in a transmission electron microscope.[1,2] Such near-edge features, recorded using the technique of electron energy loss spectroscopy (EELS), essentially involve transitions from atomic-like core levels to unoccupied states just above the Fermi level and have been shown to provide information concerned with the local chemical and structural environments of particular atoms within a solid state sample.[3—6]

Under the conditions of small momentum transfer and small sample thickness the interpretation of ELNES follows along similar lines to that of *X*-ray absorption near-edge structure (XANES). From single-electron theory the core-edge intensity is directly proportional to the projected density of unoccupied states of the appropriate symmetry provided the matrix element overlap factor, which describes the coupling between the initial and final states, varies slowly over the energy region of interest.[7] In reality the core-edge intensity may be modified by many body effects, such as the relaxation of the unexcited electrons in response to the production of a core hole as well as excited electron-core hole interactions. For the routine application of EELS to solid state analysis it is desirable to identify certain ELNES 'fingerprints' which reflect the local site symmetry around the atom undergoing the excitation, thereby supplementing the information obtained from quantitative chemical analysis.[8,9]

In previous studies[10,11] we have reported measurements of the ELNES associated with the various core loss edges in the EELS spectrum of the mineral rhodizite, the compositional formula of which was confirmed to be[10] $(K_{0.46}Cs_{0.36}Rb_{0.06}Na_{0.02})_{\Sigma 0.90}Al_{3.99}Be_4$ $(B_{11.35}Be_{0.55}Li_{0.02})O_{28}$. By comparison with the results of real space multiple scattering calculations, obtained using the 'ICXANES' computer code of Vvedensky *et al.*,[12] we were able to confirm the octahedral co-ordination of aluminium and tetrahedral co-ordination of beryllium and boron in this structure. This was achieved using a cluster consisting of a single shell of oxygen neighbours surrounding a central absorbing atom. This approach appears to be justified by consideration of the fact that the O^{2-} ion is a very strong backscatterer and produces considerably more structure than other species, which, in view of the comparatively large unit cell of rhodizite[13] containing many different atoms, would suggest that many of the gross features in the ELNES are due to the nearest neighbour oxygen shell. Furthermore, Knapp *et al.*[14] have shown that the transition metal K-edges of complex oxides essentially reflect the local co-ordination of the transition metal atom to oxygen. These findings suggest the existence of characteristic ELNES fingerprints, especially in the case of metal oxyanion units. Our Communication confirms this fact by comparison of the rhodizite spectra with those obtained from another mineral where, on the basis of prior *X*-ray structure determination, the co-ordination of the light elements is known to be the same.

Our reasons for choosing chrysoberyl, Al_2BeO_4, are several. It is a naturally occurring mineral which is resistant to electron beam induced damage and contains aluminium octahedrally, and beryllium tetrahedrally, co-ordinated to oxygen.[15] The measurements presented here were performed on a dedicated scanning transmission electron microscope fitted with a sector field spectrometer and parallel recording

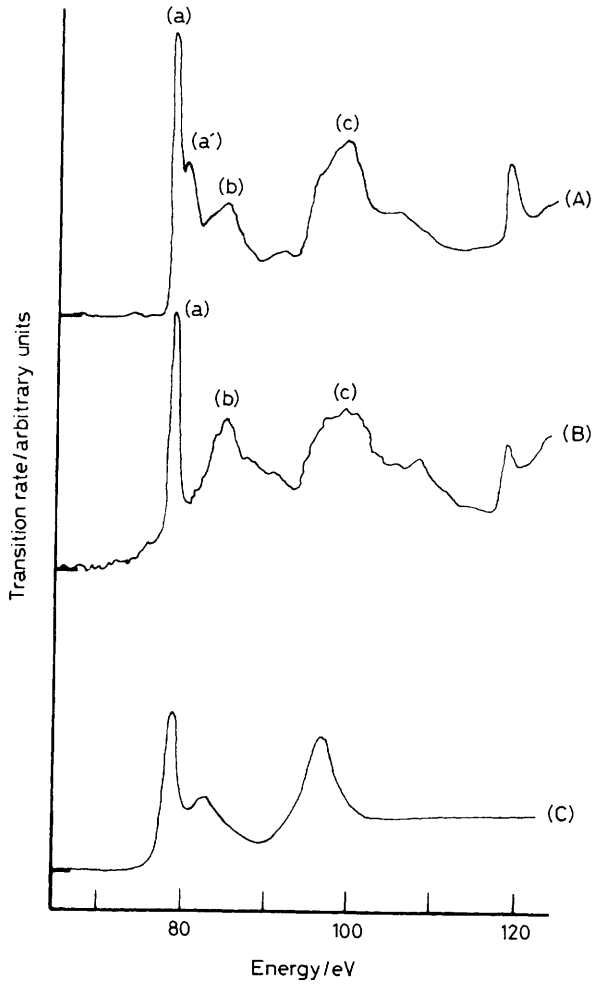

Figure 1. The EELS spectrum of the aluminium $L_{2,3}$-edge in (A) chrysoberyl and (B) rhodizite after background subtraction. Peak positions are given in Table 1. (C) The results of ICXANES calculations for aluminium octahedrally co-ordinated to a single shell of oxygen neighbours.

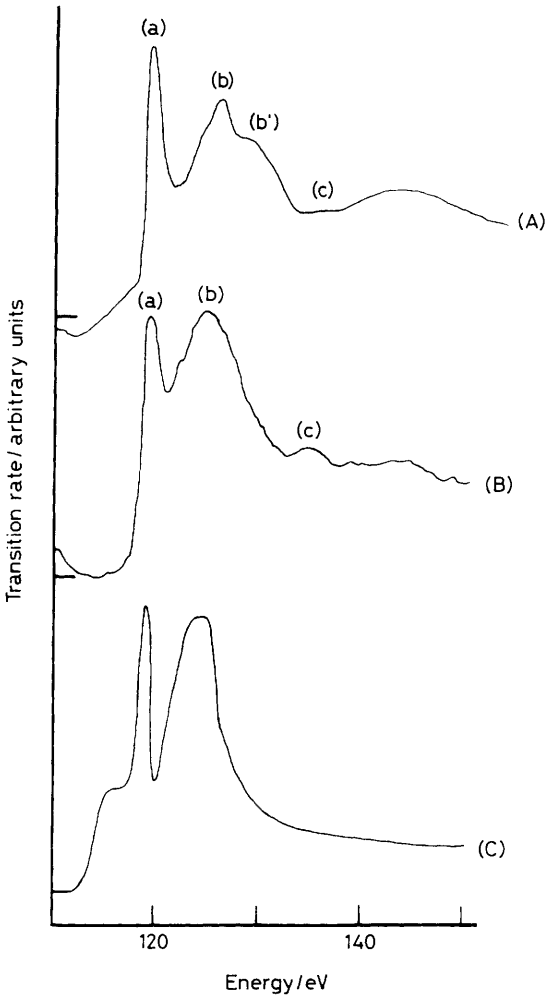

Figure 2. The EELS spectrum of the beryllium K-edge in (A) chrysoberyl and (B) rhodizite after background subtraction. Peak positions are given in Table 1. (C) The results of ICXANES calculations for beryllium tetrahedrally co-ordinated to a single shell of oxygen neighbours. Core hole effects have been included by use of the $(Z + 1)^*$ approximation for the absorbing atom; see text for details.

array, described in detail elsewhere.[16] Samples were prepared by grinding in acetone and dispersing on holey carbon films supported on electron microscope grids. The recording conditions were the same for both sets of spectra. Deconvolution so as to remove the effects of multiple inelastic scattering produced little difference in the near-edge region indicating that the specimen areas under study were quite thin. The contribution of multiple inelastic scattering to the observed ELNES is most apparent ~25 eV (or one plasmon loss) above the edge onset. It is therefore better in the first instance to concentrate on the near-edge region.

In Figure 1, curve (A) shows the aluminium $L_{2,3}$-edge of chrysoberyl after subtraction of the background, while curve (B) reveals the equivalent spectrum for rhodizite. Both spectra exhibit three main features, peaks (a), (b), and (c), the energies of which are given in Table 1. The aluminium $L_{2,3}$-edge of chrysoberyl exhibits a further feature (a'), on the high energy side of peak (a); however, the two spectra show considerable qualitative agreement suggesting that the gross structure, peaks (a), (b), and (c), arises from the octahedrally co-ordinated oxygen nearest neighbours. This is supported by

Table 1. Energies of the significant features in the EELS Al $L_{2,3}$- and Be K-spectra of chrysoberyl and rhodizite in eV.[a]

	Peak	Al $L_{2,3}$-	Be K-
Chrysoberyl	(a)	78.8 (1.2)	119.3 (2.1)
	(a')	80.2 (2)	—
	(b)	84.9 (4)	125.9 (5.0)
	(b')	—	128.7 (4)
	(c)	99.3 (8)	135.7 (3)
Rhodizite	(a)	79.1 (1.1)	119.1 (2.0)
	(b)	85.2 (2.3)	124.6 (5.4)
	(c)	99.0 (7)	134.9 (2)

[a] Peak positions, on an absolute energy scale, are accurate to within ±0.2 eV. The numbers in brackets give the full width at half maximum (FWHM) in eV, which have been derived either by direct measurement or by use of a Gaussian fitting procedure.

comparison with curve (C) which shows the previously published results of our ICXANES calculations for aluminium octahedrally co-ordinated to a single shell of oxygen neighbours. The calculation successfully models the features (a), (b), and (c); the additional structure which is apparent in both experimental spectra must therefore, to a greater extent, originate from the outer lying shells of atoms surrounding the central absorbing atom. As discussed,[10] the initial peak (a) is present in the calculation assuming octahedral co-ordination, but is completely absent if we assume tetrahedral co-ordination. Furthermore, in the octahedral case, we observed that the initial peak(a) may only be reproduced by the inclusion of $p \rightarrow s$ transitions as well as $p \rightarrow d$ transitions. This is in agreement with the work of Tossell[17,18] who calculated the molecular orbital (MO) energy levels for the octahedral and tetrahedral oxyanions of silicon, aluminium, and magnesium. In each of the three octahedral cases, the lowest unoccupied molecular orbital (LUMO) has central atom s character, whereas in the tetrahedral cases the LUMO consists of mainly d character. Aluminium $L_{2,3}$ spectra of α-Al_2O_3 measured using EELS[6] and *X*-ray absorption spectroscopy (XAS)[19—21] are in close correspondence with our Al $L_{2,3}$ spectrum of chrysoberyl which is to be expected since again aluminium is in octahedral co-ordination to oxygen. However, Balzarotti *et al.*[21] assign the strong initial peak (a), to an exciton which is seemingly refuted by our multiple scattering calculations which do not include any allowance for the core hole (this may be done by employing an excited state configuration for the central absorbing atom).[11] It should be noted that this does not rule out the possibility of excitonic enhancement of the peak. In terms of MO theory[17] we may therefore assign peaks (a) and (a') to transitions to the $7a_{1g}$ and $2t_{2g}$ orbitals respectively.

Figure 2, curve (A), shows the background-subtracted beryllium K-edge of chrysoberyl, curve (B) again showing the equivalent spectrum for rhodizite. Fitting a background is problematical, since this edge lies on the tail of the aluminium $L_{2,3}$-edge. However, if we use the same fitting procedure for both edges,[10] then we again find that both spectra are qualitatively very similar, exhibiting three main features (a), (b), and (c) in the near-edge region, the energies of which are given in Table 1. Peak (a) is very similar in both spectra, while peak (b) exhibits considerably more structure in the case of chrysoberyl, notably a high energy shoulder (b'). Peak (c), meanwhile, is only weakly visible in chrysoberyl. Curve (C) shows the previously published results of our ICXANES calculations for beryllium surrounded by a single shell of tetrahedrally co-ordinated oxygen neighbours. As previously discussed,[11] the initial peak (a) could be successfully modelled

only if core hole effects were accounted for by use of the $(Z + 1)^*$ approximation for the central absorbing beryllium atom. The conclusion that the observed structure is characteristic of a BeO_4 tetrahedral unit is also supported by the measurements of Hofer[22] who investigated the beryllium K-edge spectra of BeO and Be_2SiO_4 (both of which possess tetrahedral co-ordination of oxygen to beryllium[15]) and found very similar near-edge structures to those in Figure 2. MO theory[23] predicts that the lowest unoccupied MO of a BeO_4^{6-} cluster is the $5t_2$ orbital of predominately Be 2p character.

In conclusion, we have indicated the possibilities for the identification of ELNES fingerprints which allow for the rapid assignment of nearest neighbour co-ordinations in complex structures. By comparing the ELNES from a variety of 'known' structures, together with the modelling of near-edge features using multiple scattering calculations, it should be possible to build up a systematic library of ELNES spectra for routine use in microanalysis.

We thank Dr. Ferdinand Hofer for invaluable discussions. We gratefully acknowledge support from the Royal Society (for a fellowship to R. B.), the S.E.R.C., and the Max-Planck-Gesellschaft.

Received, 21st January 1989; Com. 9/00331B

References

1 R. F. Egerton, 'Electron Energy Loss Spectroscopy in the Electron Microscope,' Plenum Press, New York, 1986.
2 O. L. Krivanek, C. C. Ahn, and R. B. Keeney, *Ultramicroscopy*, 1987, **22**, 103.
3 B. G. Williams, *Prog. Solid State Chem.*, 1987, **17**, 87; J. M. Thomas, B. G. Williams, and T. G. Sparrow, *Acc. Chem. Res.*, 1985, **18**, 324.
4 M. Isaacson in, 'Microbeam Analysis in Biology,' eds. C. P. Lechene and R. R. Warner, Academic Press, New York, 1979.
5 J. Tafto and J. Zhu, *Ultramicroscopy*, 1982, **9**, 349.
6 C. Colliex, T. Manoubi, M. Gasgnier, and L. M. Brown, *Scanning Electron Microscopy*, 1985, **2**, 489.
7 L. V. Azaroff and D. M. Pease in, '*X*-ray Spectroscopy,' ed. L. V. Azaroff, McGraw-Hill, New York, 1974.
8 F. Hofer and P. Golob, *Ultramicroscopy*, 1987, **21**, 379.
9 R. Brydson, J. Bruley, and J. M. Thomas, *Chem. Phys. Lett.*, 1988, **149**, 343.
10 R. Brydson, B. G. Williams, H. Sauer, W. Engel, Th. Lindner, R. Schlogl, M. Muhler, E. Zeitler, and J. M. Thomas, *J. Chem. Soc., Faraday Trans. 1*, 1988, **84**, 631.
11 R. Brydson, D. D. Vvedensky, W. Engel, H. Sauer, B. G. Williams, E. Zeitler, and J. M. Thomas, *J. Phys. Chem.*, 1988, **92**, 962.
12 D. D. Vvedensky, D. K. Saldin, and J. B. Pendry, *Computer Phys. Commun.*, 1986, **40**, 421.
13 A. Pring, V. K. Din, D. A. Jefferson, and J. M. Thomas, *Mineralogical Magazine*, 1986, **50**, 163.
14 G. S. Knapp, B. W. Veal, H. K. Pan, and T. Klippert, *Solid State Commun.*, 1982, **44**, 1343.
15 R. W. G. Wyckoff, 'Crystal Structures,' Interscience, New York, 1960.
16 W. Engel, H. Sauer, R. Brydson, B. G. Williams, E. Zeitler, and J. M. Thomas, *J. Chem. Soc., Faraday Trans. 1*, 1988, **84**, 617.
17 J. A. Tossell, *J. Phys. Chem. Solids*, 1975, **36**, 1273.
18 J. A. Tossell, *J. Am. Chem. Soc.*, 1975, **97**, 4840.
19 I. A. Brytov and Yu. N. Romashchenko, *Sovt. Phys. Solid State*, 1978, **20**, 384.
20 A. Balzarotti, F. Antonangeli, R. Girlanda, and G. Martino, *Solid State Commun.*, 1982, **44**, 275.
21 A. Balzarotti, F. Antonangeli, R. Girlanda, and G. Martino, *Phys. Rev. B*, 1984, **29**, 5903.
22 F. Hofer, personal communication.
23 D. J. Vaughan and J. A. Tossell, *Am. Mineral.*, 1973, **58**, 765.